Gold nanoparticle based capacitive immunosensor for detection of hepatitis B surface antigen

Elias Alipour,[a] Hedayatollah Ghourchian*[ab] and Seyed Mehdi Boutorabi[c]

A simple, rapid and label-free capacitive based immuno-biosensor was developed for the detection of the hepatitis B surface antigen (HBsAg). Two planar gold electrodes were used as capacitor plates. The surfaces of the electrodes were covered by a mixture of $HS(CH_2)_{11}(OCH_2CH_2)_3OH$ and $HS(CH_2)_{11}(OCH_2CH_2)_3COOH$ (20 : 1 weight ratio) as an insulating molecule layer. Then, the primary anti-HBsAg was immobilized on the insulating layer. After the addition of HBsAg, the distance between the plates and also the average surface area of the plates changed. The alteration of these factors led to a change in capacitance which could be used as an indicator of the antibody–antigen interaction. Also, in order to improve the sensitivity of the method, gold nanoparticles were attached to a secondary antibody. Due to the relatively large size of the particles, the thickness of the dielectric layer and thus the capacitance changed remarkably. Therefore, the detection limit was improved to about 10 ng ml^{-1}.

Introduction

Affinity biosensors fall into two general categories of labelled and label-free. Different electrochemical methods such as potentiometry,[1,2] amperometry,[3] conductimetry,[4] and impedance[5] were used as labelled methods. Capacitance measurements were used as simple, label-free and sensitive approaches.[6–12] So far these were applied for the detection of many different analytes (*i.e.* antigens, antibodies, proteins, DNA fragments, and heavy metal ions).[7] Capacitive immunosensors are usually developed based on the alkylthiol-coated gold electrodes having the sandwich type structure electrode–linker–antibody. The capacitive transducer is based on the theory of the electrical double layer,[13] which, in principle, can be described as a build up of two conducting phases: a metal surface and the electrolyte solution. A change in the capacitance is expected when the analyte binds to the surface.[14] Biological interactions often alter the dielectric properties due to, for example, conformational changes, changes in the charge distribution and the distance between the two phases. Thus, most capacitance sensors measure the change in the dielectric properties when an analyte binds to receptors immobilized on the electrode surface. For a parallel plate capacitor, the capacitance is given by eqn (1):

$$C = \varepsilon \varepsilon_0 A / d \qquad (1)$$

where, ε represents the dielectric constant of the medium between the plates, ε_0 (8.85419 pF m^{-1}) is the permittivity of free space, A is the surface area of the plates, and d shows the distance between the plates. Thus, the capacitance increases with decreasing d and increasing A and/or ε.[15]

Biological macromolecules conjugated to gold nanoparticles retain their bioactivity.[16] Therefore, these nanoparticles are particularly attractive for biological studies due to their ease of preparation, good biocompatibility and relatively large surface area.

In the present work the surface of the gold electrodes was covered by an insulating layer of 3-ethylene glycol alkanethiols with the carboxyl functional groups at the end. Then the primary antibody was immobilized on the insulating layer. By addition of the antigens, the distance between the plates and their average surface area were changed. Alteration of these factors, which led to a change in capacitance, was used as an indicator of the antibody–antigen interaction. In order to improve the sensitivity of the method, gold nanoparticles (GNPs) were attached on a secondary antibody. Accordingly, the sensitivity and detection limit were enhanced remarkably.

Experimental

Reagents

The hepatitis B surface antigen (HBsAg), polyclonal rabbit anti-HBsAg as the primary antibody and monoclonal anti-HBsAg as the secondary antibody were gifted from PishtazTeb Company (Tehran, Iran). 3-Ethylene glycol alkanethiols of $HS(CH_2)_{11}(OCH_2CH_2)_3OH$ and $HS(CH_2)_{11}(OCH_2CH_2)_3COOH$ were purchased from Prochimia, Poland. Gold nanoparticles (GNPs), 20-nanometers in diameter, 11-mercaptoundecanoic

[a]Institute of Biochemistry & Biophysics, University of Tehran, Enghelab Ave., Tehran 1417614411, Iran

[b]Nanobiomedicine Center of Excellence, Nanoscience and Nanotechnology Research Center, University of Tehran, Tehran, Iran

[c]Pishtazteb Medical Co., Tehran, Iran

acid (MUA), N-(3-dimethylaminopropyl)-N-ethylcarbodiimide hydrochloride (EDC), N-hydroxysuccinimide (NHS), 2-(N-morpholino)-ethanesulfonic acid (MES), bovine serum albumin (BSA), potassium dihydrogen phosphate and dipotassium hydrogen phosphate were obtained from Sigma. The other chemicals were purchased from Merck and used as delivered. A solution of 1% (w/v) BSA in 50 mM phosphate buffer solution (PBS), pH 7.4, was used as a blocking buffer. The washing solution was prepared by dissolving 0.02% (v/v) Tween-20 in PBS. Various concentrations of HBsAg and anti-HBsAg were prepared by diluting the corresponding stock solutions in the PBS. The solutions were prepared in double distilled deionized water (18 MΩ, Barnstead, Dubuque, USA) and all experiments were carried out at room temperature.

Apparatus

All capacitance measurements were recorded using a LCR meter (model 8118 Hameg Co, Germany). Amperometric measurements were performed using a potentiostat/galvanostat (263A, EG&G, USA). For the capacitance measurements, a well containing two planar gold electrodes (diameter of 1 mm, Scheme 1B, yellow plates) was used as a capacitor.
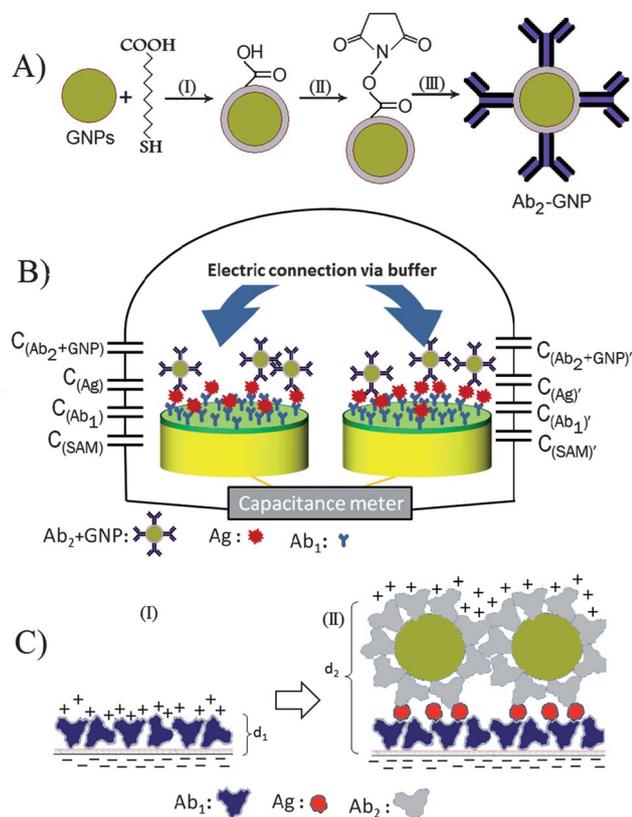
Insulating monolayer formation

In order to clean the planar gold electrode surface, the electrodes were polished carefully with 1 and 0.3 micron Al$_2$O$_3$, respectively. Thereafter, 100 μl of the alkanethiols solution (a mixture of HS(CH$_2$)$_{11}$(OCH$_2$CH$_2$)$_3$OH and HS(CH$_2$)$_{11}$(OCH$_2$CH$_2$)$_3$COOH, 20 : 1 weight ratio) in ethanol (1 mM) was added to each well and incubated overnight in order to form an insulating self-assembled monolayer (SAM) (Scheme 1B, green layer). Afterwards, the wells were rinsed thoroughly with ethanol to remove any loosely bound alkanethiol and then rinsed with PBS buffer.

Immobilization of the primary antibody

A mixed solution of NHS (0.05 M) and EDC (0.2 M) was prepared in a MES buffer at pH 6. Each couple of sensing gold plate electrodes in a well was exposed to the mixture solution for 20 min. This was required to activate the terminal carboxylic acid groups of the SAM (Scheme 1B). After that, to immobilize the primary antibody, the modified gold electrodes were incubated in 20 μl of PBS (pH 7.4) containing the primary antibody (0.5 μg ml^{-1}) for 1 h (Scheme 1B). To block any un-reacted terminal carboxylic acid groups, further incubation was done using 1% BSA in PBS as a blocking buffer. Finally, each well was carefully washed with PBS to remove any loosely non-bound Ab$_1$ or BSA.

Attachment of the secondary antibody to the gold nanoparticles

In order to adjust the pH to 8–9, the colloidal GNPs were dialyzed against a NaOH (1 mM) solution.[17] Then, 1 ml of the colloidal GNPs was mixed with 1 ml of PBS at pH 8 containing 0.02% (v/v) Tween-20 to stabilize the GNPs against aggregation.[18] Thereafter, 500 μl of MUA (2 mM) in absolute ethanol was added to 2 ml of the colloidal GNPs. This solution was gently stirred for 12 h at 4 °C. This process led to the formation of a self-assembled monolayer of MUA on the GNPs (Scheme 1A, step I). Then, the modified GNPs were centrifuged at 14 000 rpm

Scheme 1 (A) The process for attachment of the secondary antibodies to gold nanoparticles: (I) insulating monolayer formation on the GNPs *via* a SAM; (II) activation of the terminal carboxylic acid groups of the SAM *via* NHS and EDC binding; (III) connection of Ab$_2$ to the activated GNPs. (B) Representation of the capacitance measurement. The sandwiches of Ab$_1$–HBsAg–Ab$_2$ + GNPs formed on the gold electrodes (yellow) modified by a SAM of MUA (green). The equivalent capacitors on each electrode are also presented. (C) Schematic representation showing the capacitance change due to the distance increasing after the sandwich formation.
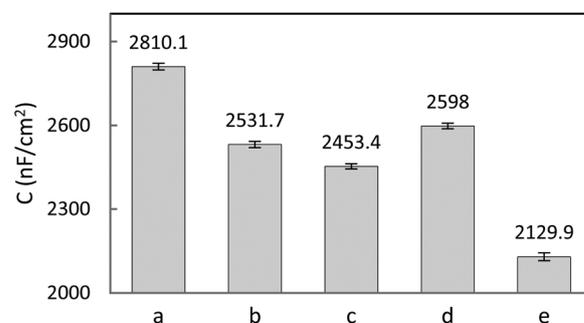

Fig. 1 Dependency of capacitance on the antibody–antigen interaction. (a): capacitance of the electrodes covered with the insulating SAM, (b): capacitance of the electrodes after immobilization of Ab$_1$, (c): same as (b) but after blocking with BSA, (d): same as (c) but after incubation with the antigen, (e): same as (d) but after incubation with Ab$_2$ + GNPs.
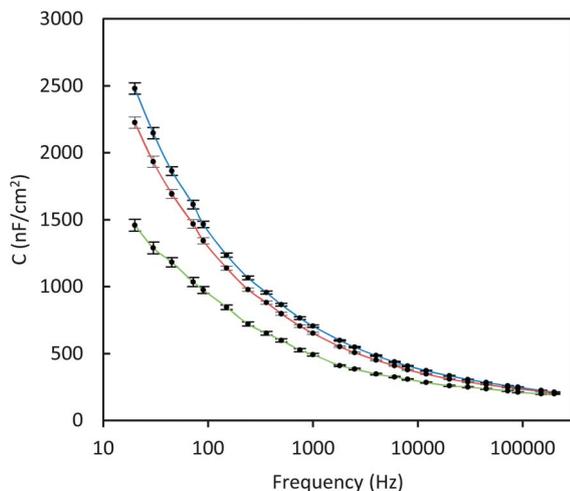
Fig. 2 Effect of frequency on capacitance. The middle line shows the capacitance change of the electrodes covered with the insulating self-assembled monolayer and primary antibody. The upper line was obtained in the same conditions as the middle line but after interaction with HBsAg. The lower line, was obtained when Ab_2 + GNPs were added to the electrodes covered by Ab_1/HBsAg. The error bars refer to the range of noise at each point.
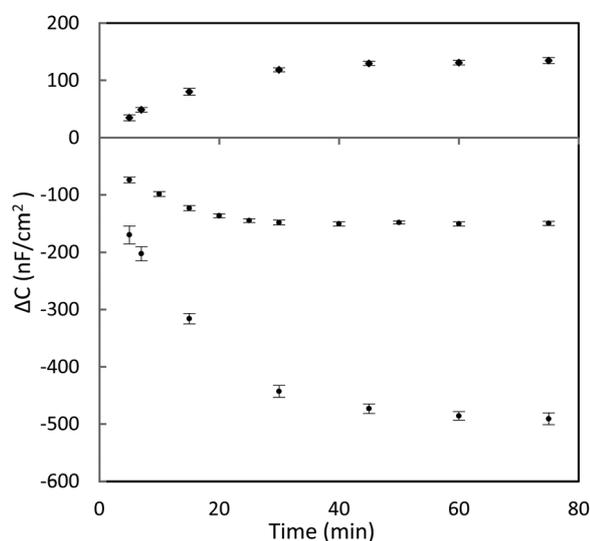

Fig. 3 Incubation times for the immobilization of Ab_1 on the insulating monolayer (middle), interaction between Ab_1 and HBsAg (80 ng ml^{-1}) (top) and interaction between HBsAg and Ab_2 + GNPs (bottom). The experiments were carried out at a frequency of 20 Hz.

for 20 min to remove the unbound MUA. The thus prepared modified GNPs were washed with 10 mM PBS (pH 7.0) and centrifuged again. The centrifugation and washing processes were repeated three times.

In order to attach the secondary antibody to the GNPs, 1 ml of the MUA-coated GNPs was mixed with 500 µl of EDC (50 mM) and 500 µl of NHS (15 mM), and was gently stirred for 10 min at room temperature. This process was necessary to activate the terminal carboxylic acid groups of the SAM (Scheme 1A, step II). The solution was centrifuged at 14 000 rpm for 20 min to remove the unbound molecules. The precipitate (activated
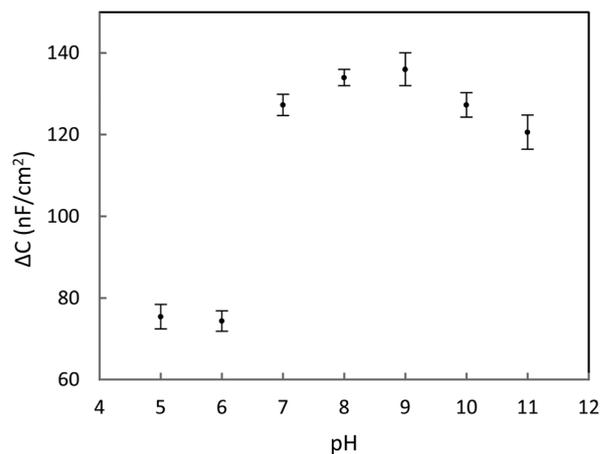

Fig. 4 Capacitance change against pH for the immobilization of the primary antibody on the insulating monolayer. The experiments were carried out at a frequency of 20 Hz and an incubation time of 20 min.
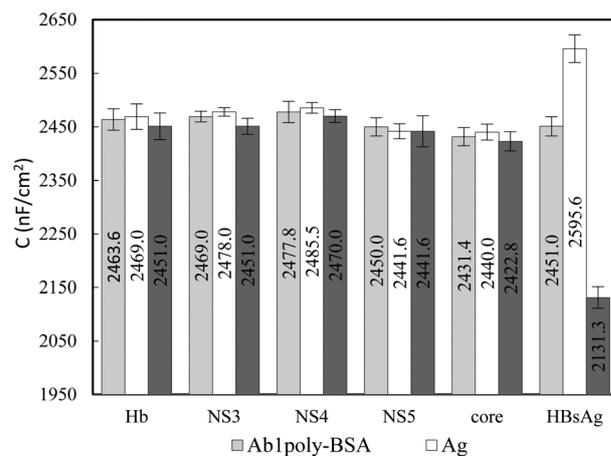

Fig. 5 Comparison of the capacitance obtained by the immunosensor for HBsAg, hepatitis C antigens (NS3, NS4, NS5, core) and hemoglobin. The planar gold electrodes covered with Ab_1 and blocked with BSA, were exposed to 10 µl of different antigens (80 ng ml^{-1}) including HBsAg, hepatitis C antigens (NS3, NS4, NS5, core) and hemoglobin. The experiments were carried out at a frequency of 20 Hz and an incubation time of 30 min.

GNPs) was re-dispersed in 1 ml of PBS (pH 7.4) containing the secondary antibody (2.5 µg ml^{-1}). This solution was incubated at room temperature for 1 h with gentle shaking on a shaker, and then kept in a refrigerator for overnight (Scheme 1A, step III). The mixture was again centrifuged at 14 000 rpm for 20 min to remove the unbound protein. The attached secondary antibody on the GNPs (Ab_2 + GNPs) was re-dispersed in 1 ml of 10 mM pH 7.4 PBS buffer. This solution was stored at 4 °C for later use.

Procedure for the detection of HBsAg

HBsAg was quantified based on a procedure called the sandwich type immune-reaction (Scheme 1B). The prepared electrodes (gold plates coated with polyclonal rabbit anti-HBsAg) were incubated in 10 µl of HBsAg for 1 h. During this period an
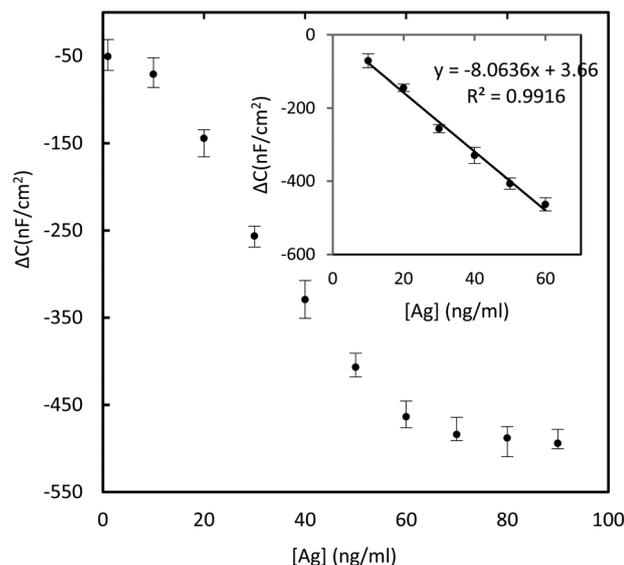
Fig. 6 Calibration curve for the detection of HBsAg. Each point is the mean value of three measurements. The planar gold electrodes covered with Ab_1 and blocked with BSA were incubated with different concentrations of HBsAg, then with Ab_2 + GNPs at the optimized conditions.

immuno-reaction between the immobilized anti-HBsAg and the free HBsAg took place. Then, the well was washed with the PBS buffer and dried under a nitrogen flow. Formation of the immuno-complex changes the distance between the plates of the capacitor and their average surface area.

Alteration of these factors will lead to a change in the capacitance according to eqn (1). The amount of change in the capacitance could be used as an indicator showing the antigen concentration. In order to improve the sensitivity and detection limit of the method, the immuno-complex was incubated in 10 μl of the Ab_2 + GNPs solution at 37 °C for 1 h to obtain the Ab_1–HBsAg–Ab_2 + GNPs immuno-sandwich (Scheme 1B). Formation of the immuno-sandwich makes more changes to the distance between the plates of the capacitor and their average surface area as illustrated in Scheme 1C. This, in turn, led to a bigger change in the capacitance (eqn (1)), which could be used as a more precise indicator for the antigen concentration. To remove the non-specific binding, the well was washed with the PBS buffer and then the capacitance was measured.

Results and discussion

Verifying the attachment of the secondary antibody on the GNPs

UV-Vis spectrophotometric data showed an absorption peak at 521 nm for the GNPs before modification. This peak was shifted to 530 nm after the self-assembling of MUA on the GNPs. This red-shift is usually attributed to the formation of Au–S bonds. Finally, after the attachment of the secondary antibody to the modified GNPs, the absorption spectrum of Ab_2 + GNPs was shifted further up to 535 nm. Comparison of these spectra verified the attachment of Ab_2 to the GNPs (data not shown).

Dependency of capacitance on the antibody–antigen interaction

Fig. 1 indicates the effect of each coating layer on the capacitance. By forming the insulating self-assembled monolayer on the gold electrode, it makes a stable capacitance and blocks any faradaic processes. Therefore, the capacitance set the highest level (Fig. 1, column a). According to the representation illustrated in Scheme 1B, two planar gold electrodes can act as two plates of the capacitor and the buffer between them can act as an insulating layer. By forming each layer on the gold electrodes, a new capacitor is formed with a different dielectric coefficient, thickness and surface area. At the first stage, two SAMs are formed on the left and right gold plate electrodes (C_{SAM} and $C_{SAM}*$). As shown in Fig. 1 (column a), at this stage the total capacitance (C_a) can be calculated *via* eqn (2):

$$\frac{1}{C_a} = \frac{1}{C_{SAM}} + \frac{1}{C_{SAM*}} \tag{2}$$

By immobilizing the primary antibody on the SAM, new capacitors (C_{Ab1} and $C_{Ab1}*$) were formed and placed in series with the previous one. So, we expect changes in the dielectric coefficient, thickness and surface area. But it seems that the thickness change is more than the other parameters. So, this is why the capacitance was decreased by Ab_1 immobilization (Fig. 1, column b). The total capacitance (C_b) at this stage can be calculated *via* eqn (3):

$$\frac{1}{C_b} = \frac{1}{C_{SAM}} + \frac{1}{C_{Ab_1}} + \frac{1}{C_{SAM*}} + \frac{1}{C_{Ab_1*}} \tag{3}$$

Table 1 Comparison of the analytical parameters obtained in the present work and those reported in the literature

Method	Response time (min)	Number of steps for determination	Label	Detection limit (ng ml^{-1})	Linear range (ng ml^{-1})	References
Capacitive immunosensor	30	1	Free/nano	10	10–60	This article
ELIZA	120	3	Enzyme	10	—	19
ELIZA	90	3	Enzyme	5	—	20
ELIZA	90	3	Enzyme	2–5	10–1000	21
Electrochemistry	60	3	Enzyme	7.8	20–160	22
Electrochemistry	30	2	Nanoparticle	15	50–4500	23

BSA as a blocker fills the empty spaces between the antibody molecules and condenses the molecules at the electrode surface. This makes the Ab_1 molecules more compact and decreases the contact area of the molecules with the buffer, and consequently reduces the capacitance further as observed in Fig. 1, column c. The addition of the antigen and the formation of the Ab_1–Ag complex formed new capacitors (C_{Ag} and $C_{Ag}*$), and again the dielectric coefficient, thickness and surface area changed but it seemed that the change in the surface area was predominant. Therefore, the capacitance increased (Fig. 1, column d). The capacitance at this stage (C_d) is given by eqn (4):

$$\frac{1}{C_d} = \frac{1}{C_{SAM}} + \frac{1}{C_{Ab_1}} + \frac{1}{C_{Ag}} + \frac{1}{C_{SAM*}} + \frac{1}{C_{Ab_1*}} + \frac{1}{C_{Ag*}} \quad (4)$$

Finally, the addition of Ab_2 + GNPs to the wells, again formed new capacitors ($C_{Ab2+GNPs}$ and $C_{Ab2+GNPs}*$), and the interaction between Ab_2 + GNPs and the antigen molecules significantly increased the thickness of the dielectric layer and consequently caused a decrease in the capacitance (Fig. 1, column e). The capacitance at this stage (C_e) is given by eqn (5):

$$\frac{1}{C_e} = \frac{1}{C_{SAM}} + \frac{1}{C_{Ab_1}} + \frac{1}{C_{Ag}} + \frac{1}{C_{Ag_2+GNPs}} + \frac{1}{C_{SAM*}} + \frac{1}{C_{Ab_1*}} + \frac{1}{C_{Ag*}} + \frac{1}{C_{Ag_2+GNPs*}}$$

$$(5)$$

Optimization of conditions

In order to optimize the conditions for the HBsAg measurements, the effect of factors such as frequency, incubation time and pH on the capacitance change were studied.

Frequency

As shown in Fig. 2, at lower frequencies the value of capacitance is high, but at this range of frequency the noise is high too. Disregarding ratios of signal/noise higher than 3, 20 Hz was chosen as the optimum frequency.

Incubation time

In the next step the incubation time was optimized for three stages of immunoreactions: (i) the immobilization of Ab_1 on the SAM, (ii) the interaction between Ab_1 and HBsAg, and (iii) the interaction between Ag and Ab_2 + GNPs. For optimizing the incubation time of Ab_1 immobilization, the capacitance was recorded while the activated gold plate electrodes were incubated in PBS (20 μl, pH 7.4) containing 0.5 μg ml^{-1} of the primary antibody at different times (5, 10, 15, 20, 25, 30, 40, 50, 60, and 75 min). As shown in Fig. 3 (middle curve), the optimum incubation time at this stage was 20 min. In the next step, the interaction between Ab_1 and HBsAg was optimized by incubating the immobilized Ab_1 in PBS (20 μl, pH 7.4) containing HBsAg (80 ng ml^{-1}) at different times (5, 8, 15, 30, 45, 60, and 75 min) and the change in capacitance was recorded (Fig. 3, top

curve). Finally, the immobilized Ab_1–Ag on the gold plates was incubated with 20 μl of PBS (pH 7.4) containing Ab_2 + GNPs (0.2 μg ml^{-1}) and the capacitance was recorded at different times (5, 10, 15, 20, 25, 30, 40, 50, 60, and 75 min). (Fig. 3, bottom curve). As shown, the optimum incubation time for the second and third steps was 30 and 45 min, respectively.

pH effect

The optimum pH for the immobilization of Ab_1 on the SAM was obtained. The planar gold electrodes covered with the activated SAM were exposed to PBS solutions (20 μl) containing Ab_1 (0.5 μg ml^{-1}) with different pH values (5 to 11). After washing with the PBS and blocking with BSA, the electrodes were exposed to 10 μl of HBsAg (80 ng ml^{-1}) and the capacitance was measured. As seen in Fig. 4, the optimum pH range for the immobilization of Ab_1 on the insulating monolayer was 7.0–9.5.

Specificity of the immunosensor

To control the specificity of the immunosensor toward HBsAg, it was exposed to the hemoglobin protein and also hepatitis C antigens including NS3, NS4, NS5 and the core antigen. Fig. 5 compares the capacitance obtained by the immunosensor for different interferences. As seen, a more selective and repeatable response was observed for HBsAg, relative to the capacitances recorded for the other interfering samples.

Detection of the hepatitis B surface antigen

Fig. 6 shows the calibration curve for the HbsAg quantification. As seen, the immunosensor response was linear in the HBsAg concentration range from 10 to 60 ng ml^{-1} with a regression equation of: $C(\mu F) = -8.0636\,C\,(ng\,ml^{-1}) + 3.66$, $(R^2 = 0.992)$. In Fig. 6 – inset, a calibration curve is presented for the quantification of the HBsAg concentration. Based on the slope of the calibration curve, the sensitivity was estimated to be 8.06 nF cm^{-2} ng ml^{-1}. Also, the detection limit was estimated to be 10 ng ml^{-1} based on a signal to noise ratio (S/N) of 3. The relative standard deviation of the immunosensor response to 10 ng ml^{-1} HBsAg was 8.3% for three successive measurements.

Finally, the analytical characteristics of the developed HBsAg immunosensor were compared with the other HBsAg capacitive immunosensors reported in ref. 19–23 (Table 1). As seen, besides the simplicity of the method and no requirement for a label, the response time and the number of steps for the determination of HbsAg were improved satisfactorily. In addition, the detection limit and linear range of the immunosensor were comparable with the other reported capacitive immunosensors.

Determination of HBsAg in real human serum

In order to measure the feasibility of the proposed immunosensor for clinical analyses, a human serum specimen was diluted in phosphate buffer solution (pH 7.4) and examined by the proposed immunosensor. The results obtained by the immunosensor (mean values of three replicated measurements 14 ± 0.4 ng ml^{-1}) were in agreement with that acquired by the standard ELISA (15 ng ml^{-1}) method.

Conclusion

A label-free immunosensor for the determination of HBsAg was developed and the operational parameters such as pH, frequency and incubation times were optimized. By incubating the immunosensor with HBsAg followed by Ab_2 + GNPs, a sandwich of Ab_1–HBsAg–Ab_2 + GNPs was formed on the gold electrodes. This composition changed the dielectric coefficient, thickness and surface area of the capacitor. Using a relatively big size of gold nanoparticles it seems that the thickness of the dielectric layer was predominant. This modification could improve the detection limit of the system to lower concentrations. It seems that the system has the ability to be used as a platform for other antigens too. Therefore, the study for further enhancement and commercialization of the system is in progress in our laboratory.

Acknowledgements

References

1 D. Tang, R. Yuan, Y. Chai Dai, J. X. Zhong and Y. Liu, *Bioelectrochemistry*, 2004, **65**, 15–22.

2 R. F. Taylor, I. G. Marenchic and R. H. Spencer, *Anal. Chim. Acta*, 1991, **249**, 67–90.

3 A. Ramanaviciene and A. Ramanavocous, *Biosens. Bioelectron.*, 2004, **20**, 1076–1082.

4 K. Yagiuda, A. Hemmi, S. Ito and Y. Asano, *Biosens. Bioelectron.*, 1996, **11**, 703–707.

5 B. Kuan Chun, *Microelectron. J.*, 2006, **37**, 1419–1423.

6 C. Berggren, B. Bjarnason and G. Johansson, *Biosens. Bioelectron.*, 1998, **13**, 1061–1068.

7 I. Bontidean, C. Berggren, G. Johansson, E. Csöegi, B. Mattiasson, J. R. Lloyd, K. J. Jakeman and N. L. Brown, *Anal. Chem.*, 1998, **70**, 4162–4169.

8 C. Berggren and G. Johansson, *Anal. Chem.*, 1997, **69**, 3651–3657.

9 I. Bontidean, J. Ahlqvist, A. Mulchandani, W. Chen, W. Bae, R. Mehra, A. Mortari and E. Csöegi, *Biosens. Bioelectron.*, 2003, **18**, 547–553.

10 S. Q. Hu, Z. M. Xie, C. X. Lei, G. L. Shen and R. Q. Yu, *Sens. Actuators, B*, 2005, **106**, 641–647.

11 W. Limbut, P. Kanatharana, B. Mattiasson, P. Asawatreratanakul and P. Thavarungkul, *Biosens. Bioelectron.*, 2006, **22**, 233–240.

12 W. Limbut, P. Kanatharana, B. Mattiasson and P. Asawatreratanakul, *Anal. Chim. Acta*, 2006, **561**, 55–61.

13 P. T. Kissinger and W. R. Heineman, *Laboratory Techniques in Electroanalytical Chemistry*, Marcel Dekker, New York, 1996.

14 M. D. Porter, T. B. Bright, D. Allara and C. E. D. Chidsey, *J. Am. Chem. Soc.*, 1987, **109**, 3559–3568.

15 B. Kang, U. Yeo and K. Yoo, *Biosens. Bioelectron.*, 2010, **25**, 1592–1596.

16 Y. Xiao, H. X. Ju and H. Y. Chen, *Anal. Chim. Acta*, 1999, **391**, 73–82.

17 N. Nath and A. Chilkoti, *J. Am. Chem. Soc.*, 2001, **123**, 8197–8202.

18 K. Aslan and V. H. Pérez-Luna, *Langmuir*, 2002, **18**, 6059–6065.

19 R. Ma, J. Du, J. Huang and C. Wu, *Biochem. Biophys. Res. Commun.*, 2007, **361**, 537–542.

20 B. Min, N. Kim, E. Jang, C. Shin, S. Lee, Y. Park, J. Hwang, S. Jeong, N. Kim and D. Lee, *Biochem. Biophys. Res. Commun.*, 2013, **431**, 92–97.

21 W. Kim, Y. Jo, E. Choi and B. Kim, *J. Immunol. Methods*, 1989, **125**, 273–278.

22 D. Tang, R. Yuan, Y. Chai, J. Dai, X. Zhong and Y. Liu, *Bioelectrochemistry*, 2004, **65**, 15–22.

23 D. Tang, R. Yuan, Y. Chai, Y. Fu, J. Dai, Y. Liu and X. Zhong, *Biosens. Bioelectron.*, 2005, **21**, 539–548.